Expression of normal and truncated forms of human endoglin

Ulla RAAB[1], Beatriz VELASCO, Pedro LASTRES, Ainhoa LETAMENDÍA, Carmela CALÉS, Carmen LANGA, Esther TAPIA, Juan Pedro LÓPEZ-BOTE, Eduardo PÁEZ and Carmelo BERNABÉU[2]

Centro de Investigaciones Biológicas, Consejo Superior de Investigaciones Científicas (CSIC), Velazquez 144, 28006 Madrid, Spain

Endoglin is a transmembrane glycoprotein 633 residues in length expressed at the surface of endothelial cells as a disulphide-linked homodimer; the specific cysteine residues involved in endoglin dimerization are unknown. Mutations in the coding region of the endoglin gene are responsible for hereditary haemorrhagic telangiectasia type 1 (HHT1), a dominantly inherited vascular disorder. Many of these mutations, if translated, would lead to truncated forms of the protein. It is therefore of interest to assess the protein expression of different truncated forms of endoglin. Infections *in vitro* or *in vivo* with recombinant vaccinia virus, as well as transient transfections with expression vectors, were used to express normal and truncated forms of endoglin. Truncated mutants could be classified into three different groups: (1) those that did not produce stable transcripts; (2) those that produced stable transcripts but did not secrete the protein; and (3) those that secreted a soluble dimeric protein. This is the first time that a recombinant truncated form of endoglin has been found to be expressed in a soluble form. Because a chimaeric construct encoding the N-terminal sequence of platelet/endothelial cell adhesion molecule (PECAM-1) antigen fused to residues Ile^{281}–Ala^{658} of endoglin also yielded a dimeric surface protein, these results suggest that cysteine residues contained within the fragment Cys^{330}–Cys^{412} are involved in disulphide bond formation. Infection with vaccinia recombinants encoding an HHT1 mutation did not affect the expression of the normal endoglin, and did not reveal an association of the recombinant soluble form with the transmembrane endoglin, supporting a haploinsufficiency model for HHT1.

Key words: endothelial cells, hereditary haemorrhagic telangiectasia 1, transforming growth factor-β, vaccinia virus.

INTRODUCTION

The gene encoding endoglin maps to chromosome 9q33–34 and has been identified as the target for the dominant vascular disorder known as hereditary haemorrhagic telangiectasia type 1 (HHT1) [1,2]. HHT is a highly penetrant autosomal dominant vascular dysplasia associated with frequent epistaxis, gastrointestinal bleeding, telangiectases and arteriovenous malformations in brain, lung and liver [3,4]. Endoglin (CD105) is a 180 kDa homodimeric membrane glycoprotein strongly expressed by human endothelial cells [5]; it is also present in syncytiotrophoblasts of full-term placenta [6], stromal cells [7,8] and certain haemopoietic cells [9–12]. Two different isoforms, L-endoglin and S-endoglin, differing in the amino acid compositions of their cytoplasmic tails, have been characterized [13,14]. Endoglin binds transforming growth factor β (TGF)-β1 and TGF-β3 with high affinity ($K_d = 50$ pM) in human endothelial cells [15] and forms heteromeric associations with the TGF-β signalling receptors types I and II [11,16]; overexpression of endoglin is able to modulate cellular responses to TGF-β [17]. The identification of the gene encoding Alk-1, a type I TGF-β receptor, as the second locus of HHT [18] suggests the involvement of the TGF-β system in the pathogenesis of this disease. Nevertheless the molecular mechanisms by which endoglin gene mutations trigger the disease remain to be unveiled. So far, more than two dozen mutations have been reported, showing a clustering of premature termination mutations in various exons coding for the extracellular domain of the protein [2,19–23]. If translated, these mutant alleles would produce a soluble protein. However, an analysis of a limited number of mutant proteins has revealed instability or intracellular degradation, in agreement with the 50 % decrease in endoglin expression at the surface of endothelial cells and activated monocytes from HHT1 patients [21]. A haploinsufficiency model has therefore been proposed that postulates that endoglin mutations lead to non-functional alleles [21,22]. This model was later confirmed by the finding of mis-sense mutations that disrupt the start codon of the gene [23]. Here we have assessed whether all truncated forms of endoglin behave similarly. We have made several cDNA constructs corresponding to truncated forms of endoglin and analysed their expression and possible interference with the normal allele by using transient transfections and infections with vaccinia virus.

MATERIALS AND METHODS

Antibodies

Mouse monoclonal antibodies (mAbs) 44G4 [anti-(human endoglin)] and HC1/6 [anti-(platelet/endothelial cell adhesion molecule) (anti-PECAM-1)] have been described previously [5,24]. Mouse mAb SN6h [12], recognizing an epitope within the fragment Glu^{26}–Gly^{230}, and mAb CLE4, specific for the fragment Gly^{331}–Gly^{586} of human endoglin [25], were obtained from the endothelial panel of the Sixth International Workshop on Human Leucocyte Differentiation Antigens. Mouse mAb 1H831, against vaccinia haemagglutinin, was kindly provided by Dr. H. Shida (Institute for Virus Research, Kyoto University, Kyoto, Japan). Mouse mAb NIH31-2 [anti-(human PECAM-1)] was obtained from the CD31 panel of the Fifth International Workshop on Human Leucocyte Differentiation Antigens. mAb NIH31-2 recognizes an epitope within the IgG domains 1–2, whereas mAb

Abbreviations used: FCS, fetal calf serum; HHT, hereditary haemorrhagic telangiectasia; mAb, monoclonal antibody; m.o.i., multiplicity of infection; PECAM-1, platelet/endothelial cell adhesion molecule 1; TGF-β, transforming growth factor β; VV, vaccinia virus.

[1] Present address: Institut für Medizinische Mikrobiologie und Hygiene, Universität Regensburg, D-93053 Regensburg, Germany

[2] To whom correspondence should be addressed (e-mail cibq120@fresno.csic.es).

HC1/6 recognizes an epitope within the IgG domains 3–6 of the human PECAM-1 antigen [26]. Rat mAb MJ7/18 [anti-(mouse endoglin)] [27] was a gift from Dr. E. Butcher (Stanford University, Palo Alto, CA, U.S.A.). Mouse mAb P4A4, recognizing an epitope within the fragment Tyr^{277}–Gly^{331} of human endoglin [25], was kindly provided by Dr. E. A. Wayner (Fred Hutchison Cancer Research Center, Seattle, WA, U.S.A.). Rabbit polyclonal antibody BN against endoglin was obtained by the immunization of rabbits with recombinant vaccinia virus (VV)-EndoL as described below.

Plasmids

The pCEXV-EndoL vector containing the human L-endoglin isoform driven by the SV40 promoter [14] was used to derive the following truncated endoglin constructs. pCEXV-Endo*276: pCEXV-EndoL was double-digested with *Bgl*II and *Mlu*I; the intervening segment was discarded, and annealed oligonucleotides (5′-GATCTGGACCACTGGAGAATAGA-3′ and 5′-CGCGTCTATTCTCCAGTGGTCCA-3′) encoding a stop codon were inserted; the resulting construct encoded residues Met^1–Asp^{276} of endoglin and corresponded to an HHT1 mutation [2]. pCEXV-Endo*437: pCEXV-EndoL was double-digested with *Sac*I and *Mlu*I; the intervening segment was discarded, and annealed oligonucleotides (5′-CATCACCACAGCGGTGAA-3′ and 5′-CGCGTTCACCGCTGTGGTGATGAGCT-3′) encoding a stop codon were inserted; the resulting construct encoded residues Met^1–Arg^{437} of endoglin. pCEXV-Endo*431: pCEXV-EndoL was double-digested with *Sac*I and *Mlu*I; the intervening segment was discarded, and the resulting plasmid was made blunt-ended and religated. The resulting construct encoded residues Met^1–Ser^{431} of endoglin plus the extension RVSTPGPHSEHAGPLHPPGGAQ. pCEXV-Endo*437 and pCEXV-Endo*431 were designed to truncate endoglin at the putative protease cleavage sequence RKK at position 437, coinciding with the boundary between exons 9 and 10. pCEXV-Endo*614: pCEXV-EndoL was digested with *Mlu*I and made blunt-ended; stop-linkers (5′-AATATTAGTTAGTTAG-3′) (Sigma) were inserted; the resulting construct lacked the cytoplasmic domain of endoglin and encoded residues Met^1–Tyr^{614}. A pcDNA/NEO plasmid encoding a soluble form of human PECAM-1 (Met^1–Lys^{601}) was generously provided by Dr. Peter J. Newman (Milwaukee, WI, U.S.A.). pCEXV-PECAM-1/Endo was generated by inserting the 0.8 kb *Bam*HI fragment of PECAM-1 cDNA into *Bgl*II-digested pCEXV-EndoL. The resulting plasmid was digested with *Xba*I, made blunt, digested with *Hin*dIII to remove the intervening sequence, and ligated with the 0.5 kb *Eco*RI/*Hin*dIII fragment of the pCEXV vector previously made blunt at the *Eco*RI site. The pCEXV-PECAM-1/Endo construct encoded residues Met^1–Ile^{214} of PECAM-1 (including the leader sequence and the first two IgG domains) fused to residues Phe^{282}–Ala^{658} of endoglin (including part of exon 7 and exons 8–14). The correct orientation and sequence were verified in each construct.

Construction of recombinant vaccinia virus

Culturing of the Western reserve strain vaccinia virus and isolation of recombinant virus was performed as described [28]. Basically, plasmids pCEXV-EndoL, pCEXV-EndoS, containing the L-endoglin or S-endoglin isoforms [14], pCEXV-Endo*276 and pCEXV-Endo*431 were digested with *Eco*RI; the resulting fragments were incubated with DNA polymerase I (Klenow fragment) and inserted into the *Sma*I site of vaccinia virus plasmid pSC11. The resulting plasmid is a vector that co-expresses the endoglin gene or its mutants inserted downstream of the vaccinia 7.5 kDa protein promoter, together with the *Escherichia coli* β-galactosidase gene under the control of the vaccinia 11 kDa protein late promoter; both genes are flanked by viral thymidine kinase sequences. Therefore, after homologous recombination, both genes were inserted into the thymidine kinase locus of the vaccinia virus genome. Control recombinant TK^- vaccinia virus (VV-TK^-) was constructed as described for the other recombinant viruses, by using the pSC11 plasmid.

Cell lines and transfections

BSC-40 (African-green-monkey kidney cells), L_6E_9 (rat myoblasts) and COS-7 cells were maintained in Dulbecco's modified Eagle's medium supplemented with 10% (v/v) fetal calf serum (FCS), 2 mM L-glutamine, penicillin (100 i.u./ml) and streptomycin (100 μg/ml) under 5% CO_2 at 37 °C. Mouse fibroblasts NCTC929 were cultured in RPMI medium containing the same supplements as above. Human umbilical vein endothelial cells were isolated from cannulated vessels incubated in the presence of collagenase for 20 min at 37 °C. Detached cells were plated in gelatin-coated flasks and grown in RPMI 1640 supplemented with 15% (v/v) FCS, 2 mM L-glutamine, penicillin (100 i.u./ml) and streptomycin (100 μg/ml), 5% (w/v) heparin and 50 μg of epidermal growth factor.

Rat myoblast stable transfectants were generated by co-transfecting pCEXV-EndoL and psV2neo at a 10:1 ratio. Plasmid DNA (10 μg) was mixed with 20 μg of Lipofectin (Gibco BRL) in serum-free medium in accordance with the protocol provided by the manufacturer. Positive clones were selected in the presence of the antibiotic G418 at 400 μg/ml. For transient transfections, COS-7 cells were incubated with 5 μg of total plasmid DNA mixed with 10 μg of Lipofectin as described above.

Immunization of mice and rabbits

Groups of 6-week-old female Balb/c mice were injected intraperitonally with 10^7 plaque-forming units of VV-Endo-L, VV-Endo*276, VV-Endo*431 or VV-TK^- in PBS, and 2 weeks later a booster injection of 5×10^8 plaque-forming units was given. After 2 weeks, sera were collected and analysed by flow cytometry. New Zealand rabbits (2.5 kg) were immunized with 10^9 plaque-forming units of either VV-Endo-L or VV-TK^- in PBS. The immunization was repeated twice with a 4-week interval; 2 weeks after the last injection, sera were collected and analysed by Western blotting.

Flow cytometry

Uninfected or vaccinia-infected [multiplicity of infection (m.o.i.) 1] cells were incubated with the indicated mAb or polyclonal antiserum (dilution 1:1.000) for 30 min at 4 °C. After two washes with PBS, FITC-labelled $F(ab')_2$ rabbit anti-mouse Ig or pig anti-rabbit Ig (Dakopatts) was added and incubation proceeded for an additional period of 30 min at 4 °C. Finally, cells were washed twice with PBS and their fluorescence was estimated with an EPICS-CS counter (Coulter Científica, Móstoles, Spain), with the use of logarithmic amplifiers.

Western blot analysis

Uninfected or vaccinia-infected (m.o.i. 1) cells were cultured at a density of 5×10^5 cells/ml, collected by centrifugation, lysed and extracts corresponding to 2×10^6 cells were subjected to SDS/PAGE [7.5% or 10% (w/v) gels] under non-reducing conditions. The supernatants of VV-Endo*276, VV-Endo*431 or VV-TK^-

infected cells (1.5 ml per 5×10^6 cells) were concentrated with a Centricon-10 concentrator (Amicon, Beverly, MA, U.S.A.) to a final volume of 100 μl; 30 μl of the concentrate was subjected to SDS/PAGE [7.5 % (w/v) gels] under non-reducing conditions. Proteins were electrophoretically transferred to nitrocellulose membranes (Millipore Corp., Bedford, MA, U.S.A.). Filters were blocked with PBS containing 5 % (w/v) milk powder for 1 h. Specific immunodetection was performed by incubation with mAb 44G4, mAb SN6h or with the rabbit polyclonal antiserum BN (anti-endoglin) overnight, followed by peroxidase-conjugated rabbit anti-mouse Ig or peroxidase-conjugated goat anti-rabbit Ig at room temperature. The presence of endoglin was revealed by using an enhanced chemiluminescence assay (ECL® detection kit; Amersham Ibérica, Madrid, Spain).

Detection of inter-species endoglin heterodimers was performed by immunoprecipitation followed by a Western blot analysis. In brief, mouse fibroblasts were infected with VV-Endo-L, lysed and subjected to immunoprecipitation with mAb P4A4 [anti-(human endoglin)] or mAb MJ7/18 [anti-(mouse endoglin)] with Protein G–Sepharose (Pharmacia Biotech, Barcelona, Spain). Immunoprecipitates were subjected to SDS/PAGE under reducing conditions, transferred to nitrocellulose membranes and incubated with the mAb MJ7/18 as described above. In this case, a peroxidase-conjugated rabbit anti-rat Ig was used to reveal the presence of mouse endoglin.

Metabolic labelling

Transiently transfected COS-7 cells were preincubated for 30 min at 37 °C in methionine/cysteine-free RPMI medium containing 1 % (v/v) FCS. Medium was removed, fresh medium containing 50 μCi/ml of [^{35}S]methionine/cysteine (ICN Biomedicals) was added and the cells were metabolically labelled at 37 °C under air/CO_2 (19:1) for 12 h. Supernatants were pre-cleared for 4 h with Protein G–Sepharose at 4 °C. Specific immunoprecipitations of the pre-cleared supernatants were performed in the presence of mAb HC1/6 (anti-PECAM-1) or mAb 44G4 (anti-endoglin), with Protein G–Sepharose. After incubation overnight at 4 °C, immunoprecipitates were isolated by centrifugation, washed twice with PBS at 4 °C and then subjected to SDS/PAGE [10 % (w/v) gel]. Detection of ^{35}S-labelled proteins was revealed with a PhosphorImager 410A and ImageQuant software (Molecular Dynamics).

Cell surface biotinylation

Transiently transfected COS-7 cells were washed at 4 °C with Hepes buffer [150 mM NaCl/5 mM KOH/1.3 mM $CaCl_2$/1.2 mM $MgCl_2$/10 mM HEPES (pH 7.4)] and left to equilibrate for 30 min at 4 °C in the same buffer. Cells were washed again and fresh Hepes buffer containing 0.5 mg/ml of sulphosuccinimidyl 6-(biotinamido)hexanoate (NHS-LC-biotin; Pierce Chemicals, Rockville, IL, U.S.A.) was added. After incubation at 4 °C for 2 h, the reaction was stopped by washing the cells twice with Hepes buffer. Specific immunoprecipitations in the presence of mAb CLE4 (anti-endoglin), mAb NIH31-2 [anti-(PECAM-1)] or mAb HC1/6 were performed as described above. Immune complexes were subjected to SDS/PAGE [7.5 % (w/v) gel] under non-reducing conditions, then electrotransferred to nitrocellulose. Filters were blocked with 5 % (w/v) milk powder in PBS for 1 h and then incubated with 2 μg/ml of streptavidin conjugated with horseradish peroxidase (Pierce Chemicals) for 2 h at room temperature. Biotinylated antigens were detected by enhanced chemiluminescence.

Receptor affinity labelling

Affinity-labelling assays were basically performed as described [29]. For cross-linking experiments, cells infected with vaccinia virus recombinants were incubated in Hepes buffer containing 0.1 % BSA with 50 pM ^{125}I-TGF-β1 (specific radioactivity 1200–2000 Ci/mmol; Amersham Ibérica, Madrid, Spain) for 4 h. Cells were washed and radiolabelled TGF-β1 was cross-linked with 0.30 mM disuccinimidyl suberate (Pierce) in Hepes buffer for 15 min at 4 °C. Cells were washed four times and solubilized in lysis buffer. The total extracts were subjected to specific immunoprecipitation. Immunoprecipitations were performed with mAb 44G4 (anti-endoglin). Detection of the ^{125}I-labelled receptors was revealed by standard autoradiography.

RNA preparation and Northern blot analysis

Total cellular RNA was isolated by using guanidinium thiocyanate/phenol/chloroform [30]. RNA samples (10 μg) were denatured and then fractionated in 1.1 % (w/v) agarose/formaldehyde gels and blotted to nitrocellulose. Membranes were hybridized in 50 % (v/v) formamide at 65 °C with excess ^{32}P-labelled probes and washed under highly stringent conditions (0.2 × SSC/0.5 % SDS at 65 °C); radiolabelled bands were detected with a PhosphorImager 410A and ImageQuant sofware (Molecular Dynamics). The probe used was the 2.4 kb *Eco*RI insert of endoglin in pcEXV-EndoS [14].

RESULTS

Expression analysis of transmembrane isoforms of endoglin by using recombinant vaccinia virus

Vaccinia is a poxvirus with the capacity to infect a wide host range *in vitro* and *in vivo* of mammalian cell types, including endothelial cells; it can be used as an expression vector producing relatively high levels of the corresponding recombinant protein [30]. To validate this expression system, we performed infection *in vitro* and *in vivo* with recombinant vaccinia virus containing both L-endoglin or S-endoglin isoforms (Figure 1). Infection of monkey kidney cells *in vitro* led to a high expression of recombinant endoglin at the cell surface, as demonstrated by flow cytometry (Figure 1A) and Western blot (results not shown) analyses. To assess the functional status of the virally encoded endoglin, ^{125}I-TGF-β_1 binding experiments were performed (Figure 1B). On infection with VV-Endo-L or with VV-Endo-S constructs, a specific radiolabelled band corresponding to L-endoglin or S-endoglin respectively was immunoprecipitated, together with minor bands corresponding to the putative TFG-β receptors types I and II, indicating that both isoforms are functionally active. In addition, infection of mice and rabbits with VV-Endo-L or VV-Endo-S resulted in the expression *in vivo* of recombinant endoglin as detected by the presence of anti-endoglin antibodies in the sera of the infected animals (Figures 1C and 1D). The specificity of these antibodies was demonstrated by flow cytometry (Figure 1C) and Western blot (Figure 1D) analyses by using myoblast transfectants expressing endoglin. These results demonstrate the expression *in vitro* and *in vivo* of the two transmembrane isoforms of endoglin by using vaccinia virus as a vector.

Expression analysis of recombinant truncated forms of endoglin

Once we had validated the vaccinia virus as an expression vector for the normal endoglin, we approached the expression of truncated forms of endoglin. Figure 2(A) represents different endoglin constructs generated that truncate the protein at exon

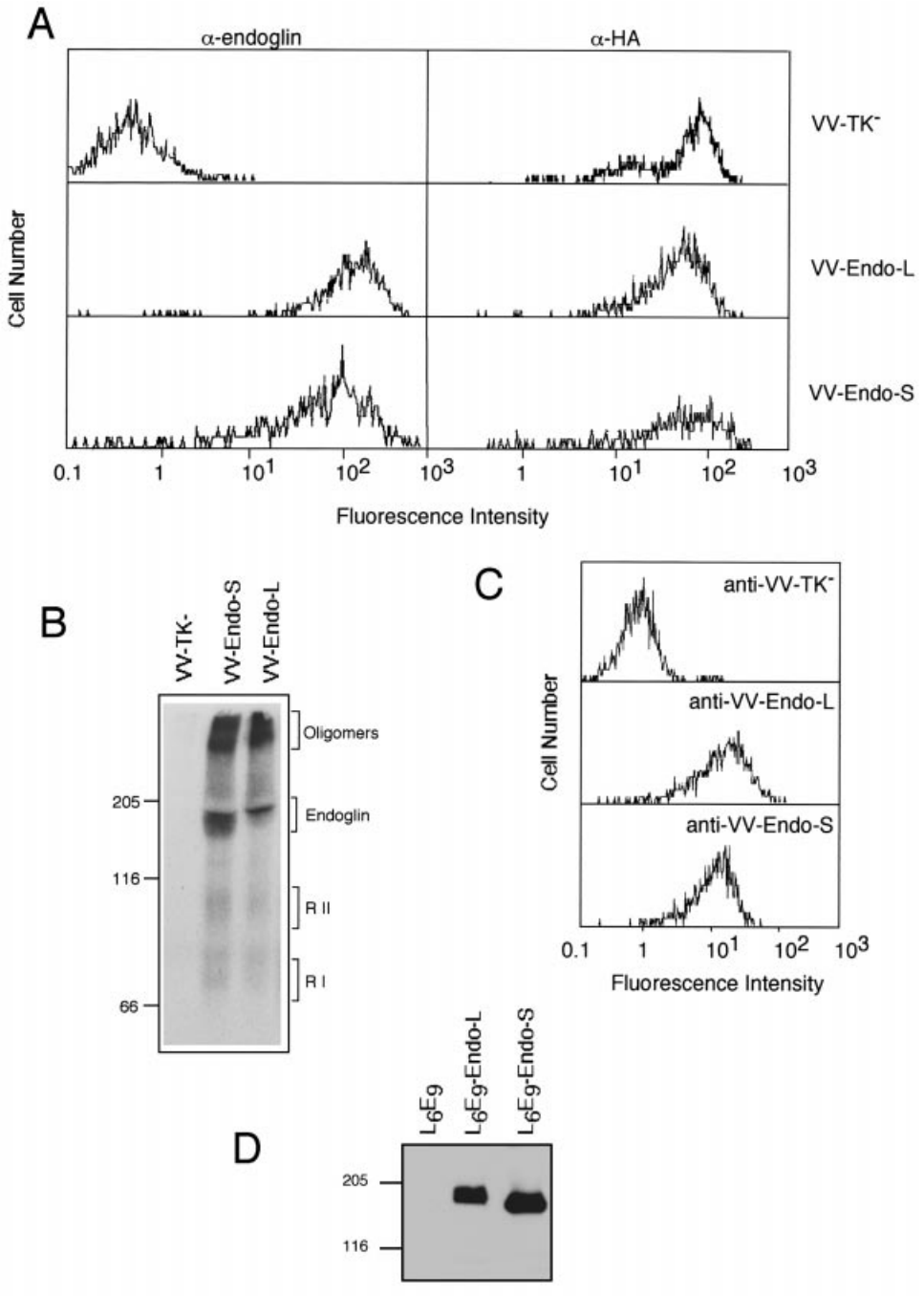

Figure 1 Characterization of endoglin expression on infection *in vitro* or *in vivo* with recombinant vaccinia viruses

(**A**) Analysis by flow cytometry of the endoglin present at the cell surface. BSC40 cells were infected with virus recombinants VV-TK$^-$, VV-Endo-L or VV-Endo-S and, 24 h after infection, were analysed by indirect immunofluorescence. Cells were incubated with either mAb 44G4 [anti-endoglin (α- endoglin)] or mAb anti-HA [anti-(vaccinia haemagglutinin); α-HA] as a control for infection, followed by incubation with FITC-labelled F(ab′)$_2$ rabbit anti-mouse Ig. (**B**) Analysis of binding of ^{125}I-TGF-β_1 to recombinant endoglin. BSC40 cells were infected with vaccinia virus recombinants (VV-Endo-L, VV-Endo-S or VV-TK$^-$) and incubated in Hepes buffer containing 0.1% BSA with 50 pM ^{125}I-TGF-β1, followed by chemical cross-linking with disuccinimidyl suberate. Cell extracts were subjected to immunoprecipitation with mAb P4A4 (anti-endoglin), followed by SDS/PAGE analysis under non-reducing conditions. ^{125}I-labelled receptors were detected by autoradiography. Bands corresponding to endoglin, endoglin oligomers and the putative TGF-β receptors I and II are indicated. The positions of molecular mass markers are indicated (in kDa) at the left. (**C**) Analysis by flow cytometry of sera from vaccinia-infected mice. Myoblast transfectants expressing L-endoglin were stained by indirect immunofluorescence with sera obtained from mice infected with VV-Endo-L, VV-Endo-S or VV-TK$^-$, followed by incubation with FITC-labelled F(ab′)$_2$ rabbit anti-mouse Ig. (**D**) Western blot analysis of serum from a vaccinia-infected rabbit. Parental myoblasts (L_6E_9) and myoblast transfectants expressing L-endoglin (L_6E_9-Endo-L) or S-endoglin (L_6E_9-Endo-S) were lysed and total extracts were transferred to nitrocellulose. Specific immunodetection was performed by incubation with the serum BN of a rabbit infected with VV-Endo-L, followed by peroxidase-conjugated goat anti-rabbit Ig ('BN' serves to identify the specific animal). Endoglin was detected by using a chemiluminescence assay. The positions of molecular mass markers are indicated (in kDa) at the left.

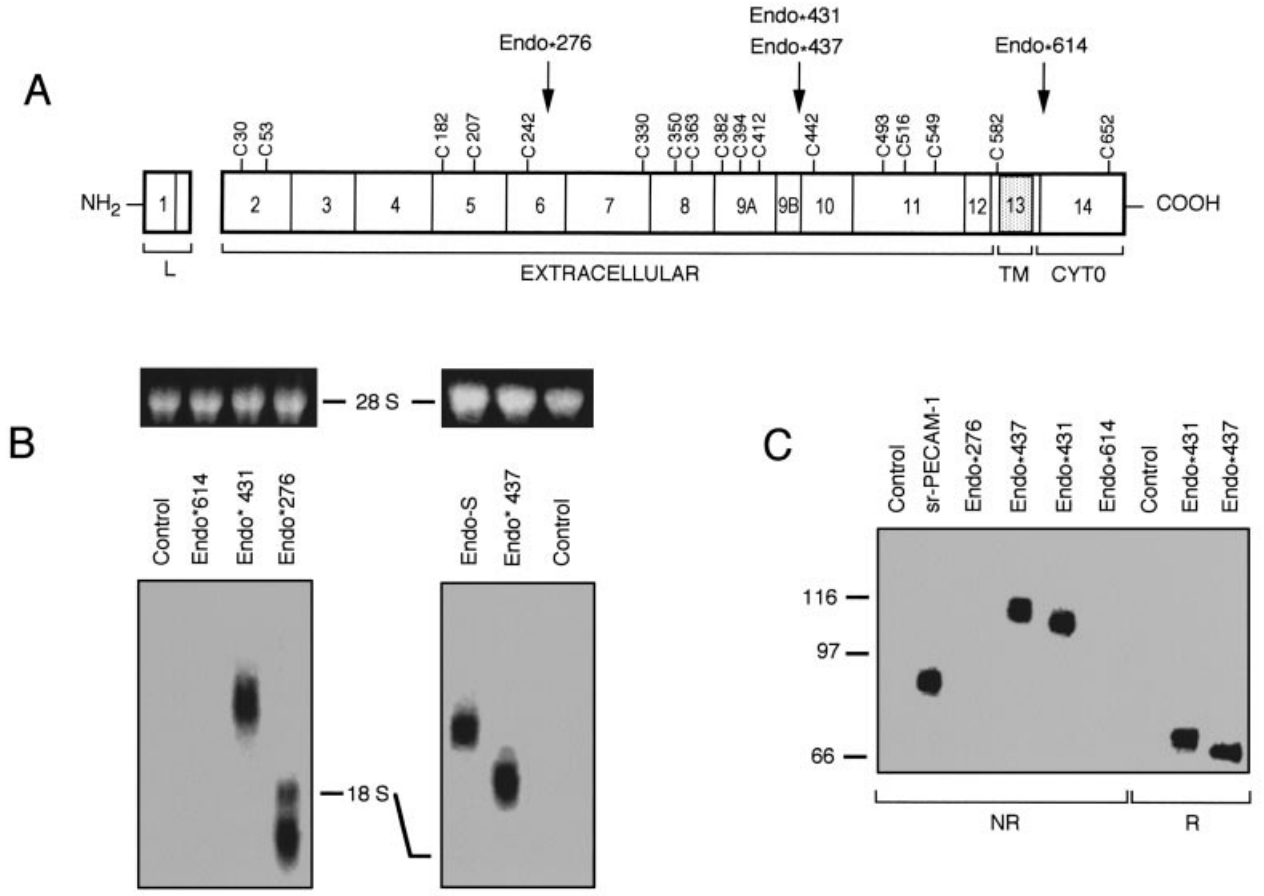

Figure 2 Expression of truncated forms of endoglin by transient transfections

(**A**) Schematic diagram of the endoglin gene, showing the locations of truncated forms of endoglin (indicated by arrows). Each exon is shown as a box with the corresponding exon number. Exons 2–12 encode the extracellular domain, exon 13 encodes the transmembrane (TM) domain and exon 14 the cytoplasmic (CYTO) domain. Only protein-encoded regions are shown. Cysteine residues (C) are numbered according to their position in the endoglin sequence. (**B**) Northern blot analysis. COS-7 cells were transfected with mutant endoglin constructs (Endo-S, Endo*276, Endo*431, Endo*437 and Endo*614); after 72 h, total cellular RNA species were isolated. RNA blots were stained with ethidium bromide to reveal the 28 S rRNA. RNA blots were hybridized with an endoglin probe; specific bands were detected by autoradiography. (**C**) Metabolic labelling. COS-7 cells were transiently transfected with mutant endoglin constructs (Endo*276, Endo*431, Endo*437 or Endo*614) with the use of Lipofectin. Cells transfected with a soluble form of PECAM-1 (sr-PECAM-1) or mock-transfected (control) were used as positive or negative controls respectively. Transfected cells were labelled metabolically with 50 μCi/ml [^{35}S]methionine/cysteine. Supernatants were subjected to specific immunoprecipitations with anti-endoglin (Endo*276, Endo*431, Endo*437, Endo*614 and control) or with anti-PECAM-1 (sr-PECAM-1) mAb. Immunoprecipitates were subjected to electrophoresis on a 10% (w/v) polyacrylamide gel under non-reducing conditions. Detection of the of ^{35}S-labelled proteins was revealed with a PhosphorImager 410A. The positions of molecular mass markers are indicated (in kDa) at the left.

6 (Endo*276), exon 9B (Endo*431 and Endo*437) or exon 13 (Endo*614). These cDNA endoglin constructs, inserted into an expression vector, were used in the transient transfection of COS cells; specific transcripts of transduced cells were detected by Northern blot analysis (Figure 2B). Constructs Endo-S, Endo*431, Endo*276 and Endo*437 each revealed a specific endoglin band with a size corresponding to the individual constructs. By contrast, Endo*614 did not show any specific transcript, suggesting the instability of its message. Next we investigated the protein expression of these constructs by metabolic labelling followed by immunoprecipitation analysis (Figure 2C). Under non-reducing conditions, polypeptides of approx. 130 and 120 kDa were immunoprecipitated from supernatants of cells transfected with Endo*431 and Endo*437 constructs respectively. In addition, the same samples electrophoretically separated under reducing conditions yielded polypeptides of approx. 66–70 kDa, which is in agreement with the predicted size of the monomeric truncated forms of endoglin. As expected from the Northern blot analysis, construct Endo*614 did not show a specific band in cell lysates or supernatants; neither did Endo*276 in spite of the presence of specific transcripts. As a control for the experiment, a soluble form of PECAM-1 of approx. 100 kDa was included. These experiments indicate that productive constructs Endo*431 and Endo*437 are able to yield stable mRNA and protein products, whereas non-productive constructs Endo*276 and Endo*614 are not.

Disulphide bonds in endoglin mutants

Immunoprecipitation analysis with Endo*431 (encoding residues Met^{1}–Ser^{431}) and Endo*437 (encoding residues Met^{1}–Arg^{437}) under reducing or non-reducing conditions (Figure 2C) indicated that cysteine residues involved in disulphide dimerization are located within the endoglin fragment Met^{1}–Cys^{412}. To analyse further the participation of this region in the dimerization process, a chimaeric construct encoding the leader sequence and the first two IgG domains of PECAM-1 fused to residues Phe^{282}–Ala^{658} of endoglin was made (Figure 3A). COS cells were transiently

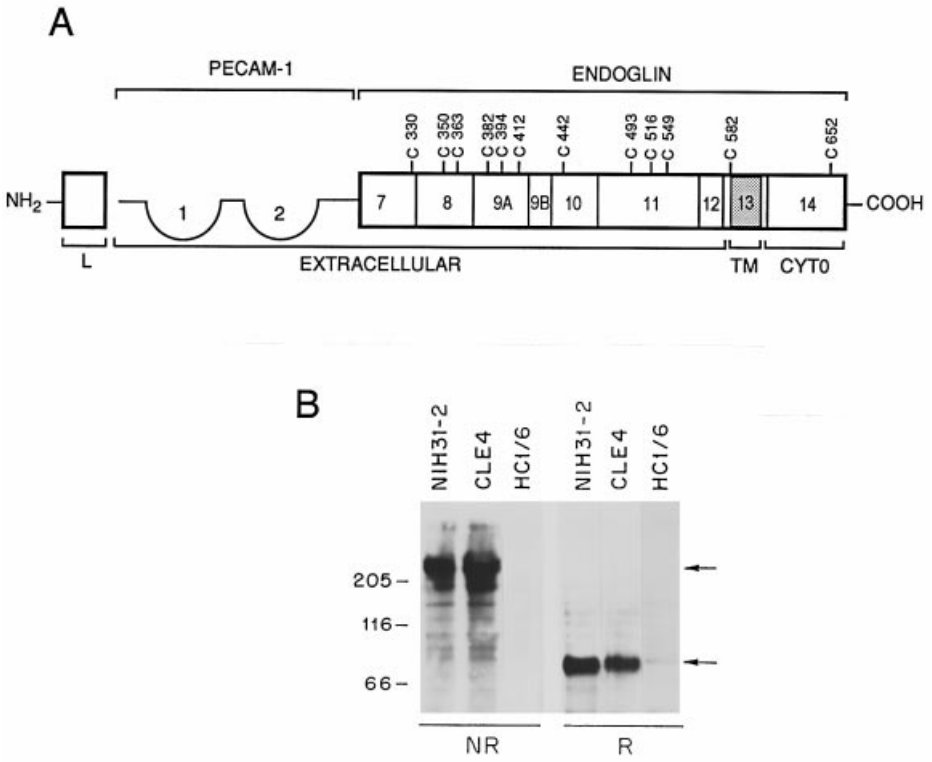

Figure 3 Expression of PECAM-1/endoglin chimaera

(**A**) Schematic representation of the predicted protein encoded by the pCEXV-PECAM-1/Endo plasmid. The N-terminal region contains the leader sequence (L) and IgG domains 1 and 2 of the human PECAM-1 followed by residues Phe^{282}–Ala^{658} of endoglin (encoded by part of exon 7 and exons 8–14). Abbreviations are as given in the legend to Figure 2. (**B**) Immunoprecipitation analysis. COS cells were transiently transfected with the pCEXV-PECAM-1/Endo plasmid, biotinylated on their surface, lysed and immunoprecipitated with mAb CLE4 [anti-(fragment Gly^{331}–Gly^{586} of endoglin)], NIH31-2 [anti-(IgG domains 1–2 of PECAM-1)] or HC1/6 [anti-(IgG domains 3–6 of PECAM-1)]. Samples were separated by SDS/PAGE under either reducing (R) or non-reducing (NR) conditions and electrotransferred to nitrocellulose membranes. Biotinylated proteins were detected with streptavidin conjugated to horseradish peroxidase by using a chemilumiscence assay. The positions of the chimaeras are indicated by arrows. The positions of molecular mass markers are indicated (in kDa) at the left.

transfected with this construct and the recombinant protein was characterized by biotinylation followed by immunoprecipitation and SDS/PAGE analysis (Figure 3B). mAb CLE4 (anti-endoglin fragment Gly^{331}–Gly^{586}) and mAb NIH31-2 [anti-(PECAM-1) IgG domains 1–2], but not mAb HC1/6 [anti-(PECAM-1) IgG domains 3–6] recognized a polypeptide of approx. 210 kDa under non-reducing conditions. When separated under reducing conditions, the recombinant protein yielded a monomer of approx. 85 kDa, indicating that disulphide bonds are responsible for the dimeric nature of the chimaera. In principle, the participation of the PECAM-1 fragment in disulphide linkages can be excluded because the complete PECAM-1 molecule is expressed as a single polypeptide [31]. Thus cysteine residues contained within the endoglin fragment Phe^{282}–Ala^{658} are probably responsible for the disulphide dimerization. This fragment and fragments Met^{1}–Arg^{437} and Met^{1}–Ser^{431}, which yield dimeric forms of endoglin, have in common six cysteine residues (Cys^{330}, Cys^{350}, Cys^{363}, Cys^{382}, Cys^{394} and Cys^{412}), suggesting their involvement in endoglin dimerization.

Recombinant vaccinia virus encoding truncated forms of endoglin

Constructs Endo*276 and Endo*431 were selected, as being representative of non-productive and productive mutant alleles respectively, for further studies with the vaccinia system. Therefore recombinant vaccinia virus containing the truncated forms Endo*276 and Endo*431 were generated. As depicted in Figure 4(A), infection of BSC-40 cells *in vitro* with these recombinants, followed by SDS/PAGE under non-reducing conditions and Western blot analyses with antibodies against endoglin, allowed the specific recognition of a soluble polypeptide of approx. 130 kDa, corresponding to the Endo*431 construct. In addition, extracts from VV-Endo*431-infected cells separated electrophoretically under reducing conditions yielded a single polypeptide of approx. 66 kDa, indicating the dimeric nature of the soluble protein. However, in the same experiment, no specific polypeptide was detected with the Endo*276 construct. This lack of recognition is apparently not due to the sole intracytoplasmic retention of the recombinant protein, because immunofluorescence staining of permeabilized cells infected with VV-Endo*276 did not reveal any cytoplasmic localization of the antigen (results not shown). Nevertheless intracytoplasmic retention associated with a rapid degradation of the protein cannot be excluded. Furthermore, the expression of the truncated proteins *in vivo* was assayed by infecting mice with the recombinant virus VV-Endo*431 or VV-Endo*276 and the presence of antibodies to endoglin was tested for in the sera of the infected animals (Figure 4B). Flow cytometry analysis with cell transfectants expressing human endoglin demonstrated the presence of specific antibodies against endoglin in the sera of animals infected with the recombinant Endo*431 but not in the sera of animals infected with the Endo*276 construct. As a positive control, a mAb against endoglin was included.

These experiments demonstrate that the truncated endoglin

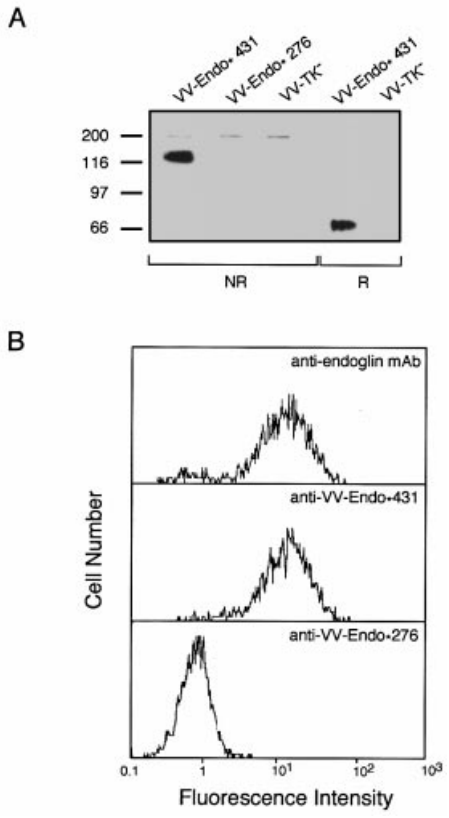

Figure 4 Characterization of vaccinia virus recombinants expressing truncated forms of endoglin

(**A**) Western blot analysis. BSC-40 cells were infected with VV-Endo*276, VV-Endo*431 or VV-TK$^-$; 12 h after infection, supernatants were collected and concentrated. The concentrates were subjected to SDS/PAGE and samples were transferred to nitrocellulose. Specific immunodetection was performed by incubation with mouse anti-endoglin antibodies followed by peroxidase-conjugated goat anti-mouse Ig. Soluble endoglin was detected by using a chemiluminescence assay. The positions of molecular mass markers are indicated (in kDa) at the left. (**B**) Flow cytometry analysis. Myoblast transfectants expressing L-endoglin (L_6E_9-Endo-L) were stained by indirect immunofluorescence with sera of mice infected with VV-Endo*276 or VV-Endo*431, followed by incubation with FITC-labelled $F(ab')_2$ rabbit anti-mouse Ig. This is a representative experiment with the use of one of six different mice sera per recombinant virus. Sera from VV-TK$^-$-infected mice yielded a negative staining similar to that of anti-VV-Endo*276 (results not shown).

form Endo*431, but not Endo*276, can be expressed on infection *in vitro* and *in vivo* by using recombinant vaccinia virus.

Effect of soluble forms of endoglin on the expression of transmembrane endoglin

As both mutant and normal endoglin alleles are present in HHT patients, it was of interest to investigate whether the soluble forms of endoglin had any effect on the expression of the normal protein. First, we used myoblast transfectants expressing the L-endoglin isoform as hosts for different recombinant vaccinia viruses (Figure 5A). Flow cytometry analysis of control cells demonstrated the relatively high expression of endoglin, which was increased further on infection with a vaccinia virus encoding the transmembrane endoglin. In contrast, infections with the vaccinia virus expressing the truncated constructs Endo*431 or Endo*276 did not affect the levels of expression of the normal endoglin. Similarly, infection with a control TK$^-$ virus did not alter endoglin expression in the transfectants. Next, we analysed primary cultures of human endothelial cells, which might be expected to be more representative of the physiological situation (Figure 5B). Again, infection with VV-Endo*431, VV-Endo*276 or VV-TK$^-$ did not affect the endogenous expression of endoglin by endothelial cells, as determined by flow cytometry. As a control for the viral infection, a mAb specific for the vaccinia haemagglutinin expressed at the cell surface of infected cells was used.

Because endoglin is a disulphide-linked dimer, there is a possibility of the formation of heterodimers between transmembrane and soluble endoglin forms at the cell surface. To test this possibility, we used the mouse fibroblast cell line NCTC, which expresses murine endoglin [7]. The existence of interspecies dimers between human and murine transmembrane endoglins could be demonstrated by using non-cross-reactive mAb against murine or human endoglin (Figure 6A). Mouse fibroblasts were infected with VV-Endo-L, lysed and immunoprecipitated with anti-endoglin antibodies. Western blot analysis of these samples revealed that the mAb MJ7/18 was able to recognize the mouse endoglin co-immunoprecipitated by an anti-(human endoglin) mAb. In contrast, no significant recognition was obtained in a parallel experiment with uninfected fibroblasts. As expected, mAb MJ7/18 clearly recognized the MJ7/18 immunoprecipitates from both infected and uninfected fibroblasts. Next, we analysed the possible formation of heterodimers between truncated and soluble endoglin forms at the cell surface. After infection with VV-Endo*431, VV-TK$^-$ or VV-Endo-L, mouse fibroblasts were analysed by immunofluorescence flow cytometry (Figure 6B). There was evidence of expression of the endogenous endoglin in all cases by the specific staining with a rat mAb against mouse endoglin. In contrast the reactivity of a mAb to human endoglin showed the expression of the recombinant transmembrane protein in VV-Endo-L-infected cells but the truncated form of endoglin could not be detected at the cell surface in the case of VV-Endo*431. In this experiment the VV-TK$^-$ construct was used as a negative control.

These results demonstrate that the expression of truncated forms of endoglin does not affect the levels of expression of the normal protein. In addition, the expression of a soluble form of endoglin does not associate with the transmembrane form at the cell surface.

DISCUSSION

Vaccinia virus is a powerful expression system that permits the appropriate transport, secretion, processing and post-translational modifications dictated by the primary structure of the recombinant protein and the cell type used as a host [32]. Here we have used this system to express human endoglin in mammalian cells. After infection *in vitro* with recombinant vaccinia virus containing L-endoglin or S-endoglin, the transmembrane antigen could be detected at the cell surface by flow cytometry and Western blot analyses. Infection of mice and rabbits *in vivo* with the same vaccinia constructs also allowed the expression of recombinant endoglin as determined by the presence of endoglin-specific antibodies in the sera of the infected animals. Furthermore, the recombinant endoglin expressed by the infected cells seems to be functional, as suggested by ligand binding assays with radiolabelled TGF-β1. The conclusive results obtained with the transmembrane forms of endoglin led us to approach the expression of truncated forms of endoglin.

Many of the mutations found in HHT1, if translated, would lead to truncated endoglin forms [2,19–23]. It was therefore of interest to assess whether truncated forms of endoglin could be expressed. Four different truncated constructs were initially

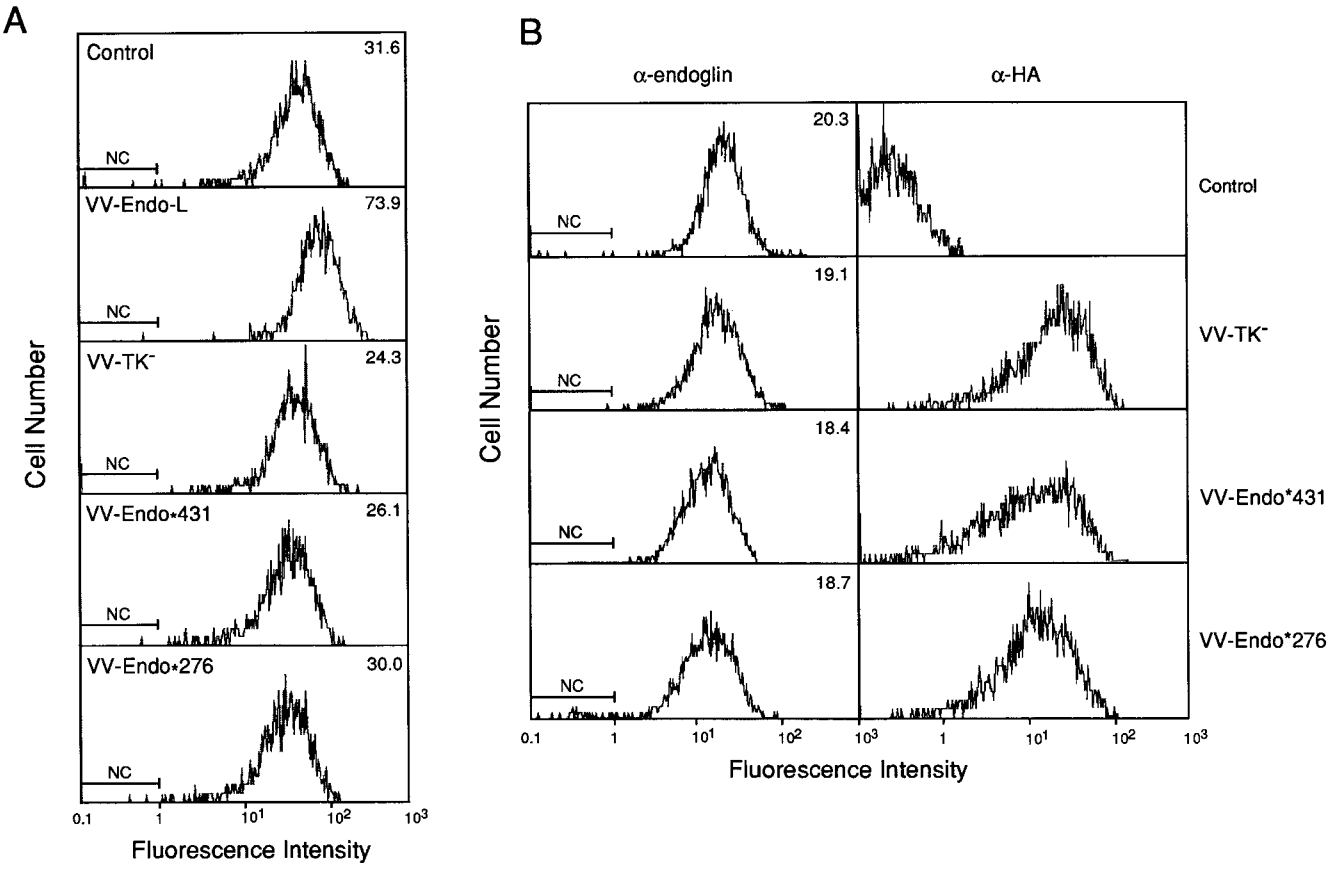

Figure 5 Expression of truncated forms of endoglin on cells expressing normal endoglin

Transfectants L_6E_9-Endo-L (**A**) or human umbilical endothelial cells (**B**) expressing human endoglin were infected with VV-TK$^-$, VV-Endo-L, VV-Endo*276 or VV-Endo*431 (m.o.i. 1), as indicated; 18 h after infection, cells were stained by indirect immunofluorescence with either anti-endoglin (44G4 mAb; α-endoglin) or anti-(vaccinia haemagglutinin) (α-HA) as a marker of infection, followed by incubation with FITC-labelled F(ab′)$_2$ rabbit anti-mouse Ig. Uninfected human umbilical endothelial cells or myoblasts (control) were included as negative controls. Cells were analysed by flow cytometry as described in the Materials and methods section. Values of mean fluorescence intensity are indicated in the upper right corner of samples stained with anti-endoglin. The limits of staining with an irrelevant antibody are indicated with a horizontal bar as a negative control (NC). Myoblast transfectants L_6E_9-Endo-L were positively stained with anti-(vaccinia haemagglutinin) as a control for infection (results not shown).

transfected in COS cells. Northern blot analyses demonstrated the absence of specific transcripts of Endo*614, containing a stop codon immediately after the transmembrane region. This is not surprising, considering that certain endoglin mutations in HHT1 patients do not produce stable endoglin transcripts [22]. The lack of mutated transcripts probably reflects an early degradation of mRNA encoding premature termination codons [33]. In contrast, Northern blot analyses demonstrated specific transcripts of Endo*276, Endo*431 and Endo*437. However, only Endo*431 and Endo*437 yielded a soluble protein in the supernatant. The Endo*276 construct contains a stop codon at the same location as an HHT1 mutant described previously [2]. The absence of a detectable protein encoded by Endo*276 is in agreement with a recent report showing the inability of several HHT1 mutations to be secreted [21], suggesting the intracellular destination and degradation of the mutant protein, if translated.

Recently, Pichuantes et al. [34] have reported the expression of different fragments of the extracellular domain of endoglin in bacteria, where the synthesized protein was targeted to inclusion bodies. However, to our knowledge, no soluble endoglin products have yet been described in mammalian cells. Here we find that both Endo*431 and Endo*437 constructs yielded secreted soluble proteins as evidenced with the use of transient transfections and recombinant vaccinia virus infections. This is the first report describing the expression of a soluble form of endoglin in mammalian cells. Given the negative results obtained with other truncated constructs [21], it is unclear why only certain mutations can be expressed at the protein level as soluble endoglin. It can be speculated that those mutations leading to a protein resembling a situation *in vivo* are more likely to be expressed. In this regard, it is of interest to note that the productive constructs Endo*431 and Endo*437 contain the stop codon close to or at a putative protease cleavage site (RKK; position 437) similar to a betaglycan sequence, postulated to be responsible for the generation of a soluble form of betaglycan [35]. In support of the relevance of the putative cleavage site of endoglin is the fact that it is located in the border between sequences encoded by exon 9B and exon 10, as well as the detection by ELISA of soluble endoglin complexes in human sera [36]. The expression of recombinant soluble endoglin might be useful in analysing the structure and function of endoglin. Because endoglin is a disulphide-linked homodimer, the soluble forms can help in elucidating the specific cysteine residues involved in disulphide bridging. Therefore the fact that constructs Endo*431 and Endo*437 and the PECAM-1/endoglin chimaera can be expressed as dimers suggests that the common endoglin fragment Cys^{330}–Cys^{412}, containing six cysteine residues,

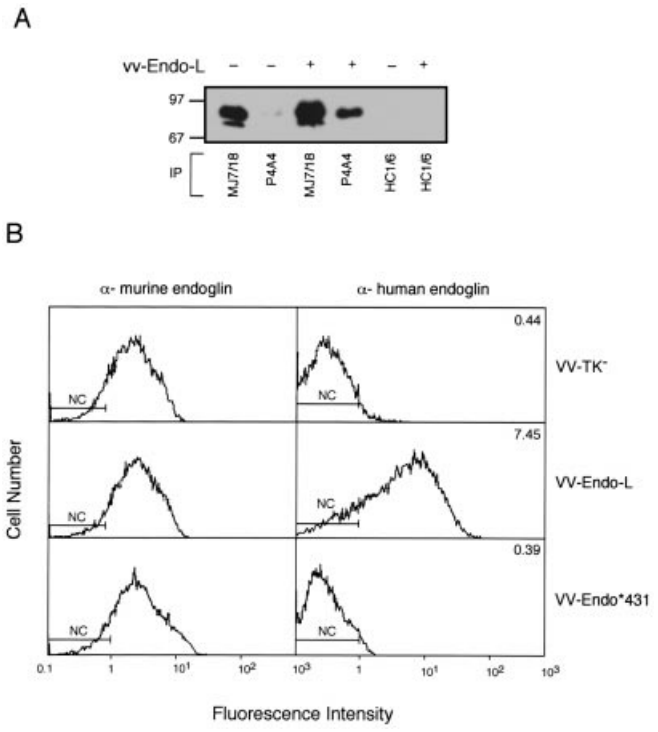

Figure 6 Inter-species dimerization between human and mouse endoglins

(**A**) Dimerization between human and mouse transmembrane endoglins. Uninfected or VV-Endo-L-infected mouse fibroblasts were lysed and subjected to immunoprecipitation (IP) with mAb P4A4 [anti-(human endoglin)], MJ7/18 [anti-(mouse endoglin)] or HC1/6 [anti-(PECAM-1)], as indicated. Immunoprecipitates were subjected to SDS/PAGE under reducing conditions, then transferred to nitrocellulose. Filters were incubated with the rat mAb MJ7/18 followed by peroxidase-conjugated rabbit anti-rat Ig. The presence of mouse endoglin was revealed by using a chemiluminescence assay. The mAb HC1/6 was used as a negative control. The positions of molecular mass markers are indicated (in kDa) at the left. (**B**) Flow cytometry analysis of mouse fibroblasts after infection with vaccinia virus recombinants expressing a truncated form of human endoglin. Mouse fibroblasts NCTC929 expressing endogenous endoglin were infected with with VV-TK$^-$, VV-Endo-L or VV-Endo*431 as indicated. After 18 h, the three recombinant viruses produced a similar cytopathic effect. Cells were then detached from the plates and stained by indirect immunofluorescence with either anti-(mouse endoglin) (MJ7/18 mAb; α-murine endoglin) or anti-(human endoglin) (SN6h mAb; α-human endoglin), followed by incubation with FITC-labelled F(ab′)$_2$ goat anti-rat Ig or rabbit anti-mouse Ig respectively. Cells were analysed by flow cytometry as described in the Materials and methods section. Values of mean fluorescence intensity are indicated in the upper right corner of samples stained with anti-(human endoglin). The limits of staining with an irrelevant antibody are indicated with a horizontal bar as a negative control (NC).

is involved in disulphide bond formation. More detailed studies by site-directed mutagenesis are required to identify the specific cysteine residues participating in endoglin dimerization.

Taken together, in the present study and previous reports [21,22] three different types of behaviour of the truncated mutants of endoglin are observed: (1) those that do not produce stable transcripts; (2) those that produce stable transcripts but do not secrete the protein; and (3) those that secrete the protein. So far, all the HHT1 mutations analysed at the protein and mRNA level have belonged to the first two types, clearly supporting a haploinsufficiency model of the disease. According to this model the mutant allele is not secreted and therefore it is unable to help or interfere in the function of the normal allele. This is in agreement with the fact that infection with VV-Endo*276, which encodes an HHT1 mutation, does not interfere with the expression of the normal allele. In the pathological situation, when the level of the normal endoglin allele does not reach a minimal threshold for its function, HHT1 is triggered. This haploinsufficiency model has been confirmed by the existence of null allele mutations in certain HHT1 patients [23]. No secreted protein has yet been reported in HHT1 patients. Nevertheless, to mimic a possible situation *in vivo*, the effect of a soluble endoglin on the expression of normal endoglin was addressed by using recombinant vaccinia virus, which allows the infection of all the cells in culture. On infection with VV-Endo*431 of endoglin-expressing cells, no association of the soluble form with the transmembrane endoglin could be detected; neither were significant differences observed in the level of expression of the transmembrane endoglin. In summary, these results suggest that potential HHT1 mutations leading to the production of a soluble form of endoglin would behave in accordance with a haploinsufficiency model. It will be of interest to analyse the possible effects of the expression *in vivo* of soluble endoglin encoded by the constructs reported here.

We thank Dr. Michelle Letarte for encouraging discussions, Dr. Peter Newman for the PECAM-1 plasmid, Francisco García Tabares for excellent technical assistance, Manuel Moreno for help with infected animals, Mónica Fontenla and Victoria Muñoz for photography, and Aurelio Hurtado for delineation. This work has been supported by grants from Comisión Interministerial de Ciencia y Tecnología (CICYT-SAF97-0034 and CICYT-BIO94-0118), Comunidad Autónoma de Madrid (CAM) and Biomed Program of the European Community (BMH4-CT95-0995).

REFERENCES

1 Fernández-Ruiz, E., St-Jacques, S., Bellón, T., Letarte, M. and Bernabéu, C. (1993) Cytogenet. Cell Genet. **64**, 204–207
2 MacAllister, K. A., Grogg, K. M., Johnson, D. W., Gallione, C. J., Baldwin, M. A., Jackson, C. E., Helmbold, E. A., Markel, D. S., McKinnon, W. C., Murrell, J. et al. (1994) Nat Genet. **8**, 345–351
3 Guttmacher, A. E., Marchuk, D. A. and White, R. I. (1995) New Engl. J. Med. **333**, 918–924
4 Shovlin, C. L. (1997) Thromb. Haemost. **78**, 145–150
5 Gougos, A. and Letarte, M. (1988) J. Immunol. **141**, 1925–1933
6 Gougos, A., St. Jacques, S., Greaves, A., O'Connell, P. J., d'Apice, A. J. F., Bühring, H. J., Bernabéu, C., van Mourik, J. A. and Letarte, M. (1992) Int. Immunol. **4**, 83–92
7 St-Jacques, S., Cymerman, U., Pece, N. and Letarte, M. (1994) Endocrinology (Baltimore) **134**, 2645–2657
8 Robledo, M. M., Hidalgo, A., Lastres, P., Arroyo, A. G., Bernabéu, C., Sánchez-Madrid, F. and Teixidó, J. (1996) Br. J. Haematol. **93**, 507–514
9 Lastres, P., Bellón, T., Cabañas, C., Sánchez-Madrid, F., Acevedo, A., Gougos, A., Letarte, M. and Bernabéu, C. (1992) Eur. J. Immunol. **22**, 393–397
10 Rokhlin, O. W., Cohen, M. B., Kubagawa, H., Letarte, M. and Cooper, M. D. (1995) J. Immunol. **154**, 4456–4465
11 Zhang, H., Shaw, A. R. E., Mak, A. and Letarte, M. (1996) J. Immunol. **156**, 565–573
12 Haruta, Y. and Seon, B. K. (1986) Proc. Natl. Acad. Sci. U.S.A. **83**, 7898–7902
13 Gougos, A. and Letarte, M. (1990) J. Biol. Chem. **265**, 8361–8364
14 Bellón, T., Corbí, A., Lastres, P., Calés, C., Cebrián, M., Vera, S., Cheifetz, S., Massagué, J., Letarte, M. and Bernabéu, C. (1993) Eur. J. Immunol. **23**, 2340–2345
15 Cheifetz, S., Bellón, T., Calés, C., Vera, S., Bernabéu, C., Massagué, J. and Letarte, M. (1992) J. Biol. Chem. **267**, 19027–19030
16 Yamashita, H., Ichijo, H., Grimsby, S., Morén, A., ten Dijke, P. and Miyazono, K. (1994) J. Biol. Chem. **269**, 1995–2001
17 Lastres, P., Letamendía, A., Zhang, H., Rius, C., Almendro, N., Raab, U., López, L. A., Langa, C., Fabra, A., Letarte, M. and Bernabéu, C. (1996) J. Cell Biol. **133**, 1109–1121
18 Johnson, D. W., Berg, J. N., Baldwin, M. A., Gallione, C. J., Marondel, I., Yoon, S.-J., Stenzel, T. T., Speer, M., Pericak-Vance, M. A., Diamond, A. et al. (1997) Nat. Genet. **13**, 189–195
19 MacAllister, K. A., Baldwin, M. A., Thukkani, A. K., Gallione, C. J., Berg, J. N., Porteous, M. E., Guttmacher, A. E. and Marchuk, D. A. (1995) Hum. Mol. Genet. **4**, 1983–1985
20 Yamaguchi, H., Azuma, H., Shigekiyo, T., Inoue, H. and Saito, S. (1997) Thromb. Haemost. **77**, 243–247
21 Pece, N., Vera, S., Cymerman, U., White, R. I., Wrana, J. L. and Letarte, M. (1997) J. Clin. Invest. **100**, 2568–2579
22 Shovlin, C. L., Hughes, J. M., Scott, J., Seidman, C. E. and Seidman, J. G. (1997) Am. J. Hum. Genet. **61**, 68–79

23 Gallione, C. J., Klaus, D. J., Yeh, E. Y., Stenzel, T. T., Xue, Y., Anthony, K. B., McAllister, K. A., Baldwin, M. A., Berg, J. N., Lux, A. et al. (1998) Hum. Mutat. **11**, 286–294
24 Cabañas, C., Sánchez-Madrid, F., Bellón, T., Figdor, C. G., Te Velde, A. A., Fernández, J. M., Acevedo, A. and Bernabéu, C. (1989) Eur. J. Immunol. **19**, 1373–1378
25 Letarte, M., Bourdeau, A., Vera, S., Pece, N., Greaves, A., Dignat-George, F., Mutin, M., Kraling, B., Linask, K., O'Brien, E. et al. (1997) in Leucocyte Typing VI (Kishimoto, T., Kikutani, H., von dem Borne, A. E. G.Kr., Goyert, S. M., Mason, D. Y., Miyasaka, M., Moretta, L., Okumura, K., Shaw, S., Springer, T. A. et al., eds.), pp. 703–708, Garland Publishing, New York
26 Yan, H.-C., Newman, P. J. and Albelda, S. M. (1995) in Leucocyte Typing V (Schlossman, S. F., Boumsell, L., Gilks, W., Harlan, J. M., Kishimoto, T., Morimoto, C., Ritz, J., Shaw, S., Silverstein, R., Springer, T. et al., eds.), pp. 1261–1262, Oxford University Press
27 Gee, A. Z. and Butcher, E. C. (1994) Gene **138**, 201–206
28 López-Guerrero, J. A., López-Bote, J. P., Ortiz, M. A., Gupta, R. S., Páez, E. and Bernabéu, C. (1993) Infect. Immun. **61**, 4225–4231
29 Massagué, J. (1987) Methods Enzymol. **146**, 174–195
30 Chomczynski, P. and Sacchi, N. (1987) Anal. Biochem. **162**, 156–159
31 Newman, P. J. (1997) J. Clin. Invest. **100** (Suppl. 11), S25–S29
32 Moss, B. and Flexner, C. (1987) Annu. Rev. Immunol. **5**, 305–324
33 Maquat, L. E. (1995) RNA **1**, 453–465
34 Pichuantes, S., Vera, S., Bourdeau, A., Pece, N., Kumar, S., Wayner, E. A. and Letarte, M. (1997) Tissue Antigens **50**, 265–276
35 López-Casillas, F., Cheifetz, S., Doody, J., Andrés, J. L., Lane, W. S. and Massagué, J. (1991) Cell **67**, 785–795
36 Blann, A. D., Wang, J. M., Wilson, P. B. and Kumar, S. (1996) Atherosclerosis **120**, 221–226

Received 10 August 1998/20 January 1999; accepted 10 February 1999